

Myxoma Virus T2 Protein, a Tumor Necrosis Factor (TNF) Receptor Homolog, Is Secreted as a Monomer and Dimer That Each Bind Rabbit TNF α , but the Dimer Is a More Potent TNF Inhibitor*

(Received for publication, February 8, 1996)

Martha Schreiber, Krishna Rajarathnam, and Grant McFadden‡

From the Department of Biochemistry, University of Alberta, Edmonton, Alberta T6G 2H7, Canada

The myxoma virus T2 (M-T2) gene expresses a secreted protein that contains significant sequence similarity to the ligand binding domains of the cellular tumor necrosis factor (TNF) receptors, specifically inhibits the cytolytic activity of rabbit TNF α and is an important virulence factor for myxoma virus infection in rabbits. M-T2 protein was overexpressed from vaccinia virus vectors, purified to apparent homogeneity, and found to specifically protect mouse and rabbit cells from lysis by rabbit TNF α at molar ratios comparable with the soluble versions of the host tumor necrosis factor receptors. M-T2 secreted from virus-infected cells is detected as both a monomer and a disulfide-linked dimer, both of which were shown by Scatchard analysis to bind rabbit TNF α (K_d values of 170 pm and 195 pm, respectively), values that are comparable with the affinities of mammalian TNFs with their receptors. In contrast to the rabbit ligand, M-T2 interacts with mouse TNF α with a much lower affinity, K_d of 1.7 nm, and was unable to inhibit the cytolytic activity of this ligand on mouse cells. Although both monomeric and dimeric forms bound rabbit TNF α with comparable affinity, the dimeric M-T2 protein was a far more potent inhibitor of rabbit TNF α , presumably because it can more effectively prevent dimerization of TNF receptors than can the M-T2 monomer.

Poxviruses are a family of double stranded DNA viruses with terminal-inverted repeats and covalently closed hairpin termini that possess genomes large enough to encode for immunomodulatory factors that inhibit or modify antiviral activities such as cytokines that are critical for the host response to infections (1–3). For example, homologs of the cellular receptors for various cytokines are encoded in various poxviral genomes, including receptor homologs of interferon- γ (IFN- γ)¹ (4–7), IFN- α/β (8, 9), interleukin-1 β (10, 11), and tumor necrosis factor (TNF) α/β (12, 13) (reviewed in Refs. 2, 3, 14, and 15). Myxoma virus, a pathogenic poxvirus of European rabbits, encodes two copies of a gene designated T2, because it is the second gene from the viral terminus, which expresses a secreted protein with significant homology to the ligand binding

domains of the TNF receptor (TNFR) gene family (12). Infection with myxoma virus results in a severe systemic infection that is invariably fatal for immunocompetent European rabbits (16, 17). However, the majority of rabbits infected with a recombinant myxoma virus in which both copies of the T2 gene were inactivated by insertional mutagenesis were able to mount an effective immune response and recover from infection (12), indicating that T2 is an important virulence factor for myxoma virus. *In vitro*, the myxoma T2 (M-T2) protein inhibits the cytolytic activities of rabbit TNF α but not mouse or human TNF α on mouse L929-8 cells (18).

TNF α plays a pivotal role in establishing and orchestrating inflammatory and immune responses to infection (19, 20). In addition, TNF α has been shown to have a number of antiviral properties. It inhibits the replication of various DNA and RNA viruses in cultured cells (21) and is directly cytolytic to cells infected with vesicular stomatitis virus (22), herpes simplex virus (23), Newcastle disease virus (24), and various adenovirus deletion mutants (25). *In vivo*, local expression of TNF α results in a dramatic attenuation of viral pathology following the infection of athymic, nude, or sublethally irradiated mice with recombinant vaccinia viruses expressing TNF α (26), and clearance of the virus is associated with elevated neutrophil numbers within 24 h postinfection (27). Moreover, the importance of TNF in an antiviral response is reinforced by the fact that adenovirus encodes four proteins that interfere with TNF signal transduction cascades (25, 28).

Biological responses to TNF are initiated when TNF α or TNF β binds and induces the oligomerization of cellular receptors (29, 30). Two different TNF receptors have been cloned and characterized, designated p55 TNFR and p75 TNFR, each of which binds and responds to both TNF α and TNF β (31–35). The TNFR superfamily, of which the M-T2 protein is a member, is characterized by the presence of multiple cysteine-rich motifs of about 40 amino acids in their extracellular amino-terminal domain (36, 37). M-T2 protein displays the greatest homology with the p75 TNFR (12), and thus rabbit TNF α and TNF β would appear to be the most likely candidates for a biological target of M-T2 protein, although other members of the TNF superfamily, including FAS ligand and CD40 ligand cannot be excluded.

The currently favored model is that M-T2 protein acts to inhibit host TNF responses by binding and sequestering either extracellular or cell surface TNF and thereby preventing the activation of cellular TNF receptors. Here we demonstrate that M-T2 protein specifically forms inhibitory complexes with rabbit TNF α and that binding is associated with the ability to inhibit the cytolytic activities of rabbit TNF α on susceptible rabbit and mouse cell lines. M-T2 protein is found to be secreted from virally infected cells as both a monomer and disulfide-linked dimer, both of which bind TNF α with similar affinities. Moreover, the dissociation constant (K_d) values for both

* This work was funded by an operating grant (to G. M.) from the National Cancer Institute of Canada. The costs of publication of this article were defrayed in part by the payment of page charges. This article must therefore be hereby marked "advertisement" in accordance with 18 U.S.C. Section 1734 solely to indicate this fact.

† Medical Scientist of the Alberta Heritage Foundation for Medical Research. To whom correspondence and reprint requests should be addressed. Tel.: 403-492-2080; Fax: 403-492-9556.

¹ The abbreviations used are: IFN, interferon; M-T2, myxoma T2; PAGE, polyacrylamide gel electrophoresis; PBS, phosphate-buffered saline; tk, thymidine kinase; TNF, tumor necrosis factor; TNFR, TNF receptor.

monomeric and dimeric M-T2 protein, assessed by Scatchard analysis, compare favorably with those of other vertebrate TNF α s with their cognate receptors. However, the dimeric form of M-T2 is far more active than the monomeric form at inhibiting the cytolytic activities of TNF α , most likely because as a divalent inhibitor, the dimer can more effectively inhibit the ability of the TNF α trimeric ligand to induce oligomerization of the cell surface TNF receptors.

MATERIALS AND METHODS

Viruses and Cells—VV-601, a derivative of vaccinia virus (strain WR) containing the *Escherichia coli lacZ* gene inserted into the vaccinia thymidine kinase (*tk*) locus has been described previously (38). As shown in Fig. 1A, VV-MT2 was engineered to overexpress and secrete the myxoma T2 protein using a synthetic late promoter (18). vMyxlac, a derivative of myxoma virus in which the *E. coli lacZ* gene is inserted between the myxoma growth factor and M9 genes (39), and vMyxt2g, in which both copies of the T2 gene are disrupted (12), are described elsewhere. Viruses were propagated in BGMK cells (provided by S. Dales) cultured in Dulbecco's modified Eagle's medium supplemented with 10% newborn calf serum (Life Technologies, Inc.). Rabbit RK-13 cells (obtained from the ATCC) were grown in Dulbecco's modified Eagle's medium supplemented with 10% fetal bovine serum (Life Technologies, Inc.); mouse L929-8 cells (provided by L. Guillet) were cultured in Iscove's modified Eagle's medium supplemented with 10% fetal bovine serum; and RL-5 cells (obtained from the National Institutes of Health AIDS research and Reference Reagent Program) were grown in RPMI media supplemented with 10% fetal bovine serum.

High Level Expression of Rabbit TNF α from a Recombinant Vaccinia Virus—The plasmid pMJ601T2RaTNF used to make a vaccinia virus that overexpresses secreted TNF α (VV-T2RaTNF) was constructed in which the rabbit TNF α cDNA sequence was placed downstream of the vaccinia synthetic late promoter (40) after the secretory leader sequence of rabbit TNF α had been replaced in frame with the secretory leader sequence of the M-T2 protein (see Fig. 1A). The plasmid pUCRATNF (18) was used as a template for the polymerase chain reaction amplification of the mature rabbit TNF sequence using the primer 5'-TGCCTATAACGGGCTCAGATCAGCTTCGGGCC containing sequence from the M-T2 leader region immediately upstream of sequence encoding the 5'-terminal mature rabbit sequence and the M-13 reverse primer 5'-AGCGGATAACAATTTCACACAGGA. Similarly, the M-T2 leader sequence containing mature rabbit TNF sequence was amplified using pMTN-6 (18) as template and the primers 5'-AGCTGATCT-GAGCCGTATAACGCCACCGGACTA and the M-13 reverse primer. Twenty rounds of amplification were carried out using 1 unit of *Taq* DNA polymerase in 50 mM KCl, 10 mM Tris-Cl, pH 8.4, 1.5 mM MgCl₂, 100 μ g/ml gelatin, 0.25 μ M dXTPs followed by gel purification of the products. The two products with overlapping termini were mixed, denatured by heating to 95 °C, and allowed to reanneal. *Taq* DNA polymerase and dXTPs were added to allow 3' extension from the overlapping termini, and a second round of polymerase chain reaction amplification of the full-length extension was carried out using M-13 reverse primers. The product was digested with *Hind*III and cloned into the *Hind*III site of pBluescript SK⁻ to create pBlueT2RaTNF. This clone was sequenced to ensure no errors had been introduced during the polymerase chain reaction amplification. A *Sall*-*Bam*HI fragment of pBlueT2RaTNF was subcloned into pMJ601 to generate pMJ601T2RaTNF. The recombinant vaccinia virus VV-T2RaTNF (strain WR) was constructed as described previously (39).

Purification of Myxoma T2 Protein and Rabbit TNF α —Myxoma T2 protein was purified from media from VV-MT2-infected BGMK cells in roller bottles (3×10^8 cells). Supernatants were prepared as described previously (18), and the media from 8–16 roller bottles was concentrated using an Amicon ultrafiltration cell to a volume of 20–30 ml and dialyzed overnight against 20 mM Tris-Cl, pH 7.5, at 4 °C. The dialyzed sample was applied to a Mono-Q anion exchange column (Pharmacia Biotech Inc.), and protein was eluted using a linear salt gradient, 0–500 mM NaCl in 20 mM Tris-Cl, pH 7.5. Fractions containing M-T2 were pooled, dialyzed against 20 mM bis-Tris, pH 6.4, and reapplied to a Mono-Q anion exchange column. Protein was eluted using a 0–500 mM NaCl salt gradient at pH 6.4. M-T2-containing fractions were analyzed for purity by silver staining of polyacrylamide gels (41).

Rabbit TNF α was purified from supernatants from VV-T2RaTNF-infected BGMK cells in roller bottles in an identical fashion, using pH 7.5 Mono-Q anion exchange chromatography followed by pH 6.4 anion exchange chromatography. The M-T2 or rabbit TNF α protein present in

the different fractions was confirmed by silver staining and quantitated by A_{280} measurements.

Generation of Polyclonal Antisera Against Myxoma T2—Antiserum was prepared by intradermally injecting rabbits with purified T2 protein (native) in Freund's complete adjuvant or with purified T2 protein resolved on a 12% SDS-polyacrylamide gel (denatured) with acrylamide as adjuvant using standard procedures (42). Immunoblots confirmed that the polyclonal antiserum recognized T2 protein from supernatants from myxoma- and VV-MT2-infected cells and did not cross-react with any proteins present in supernatants from cells infected with the T2-minus myxoma virus, (vMyxt2g) or control VV-601.

Quantitation of M-T2 Protein Secreted from Virally Infected Cells—Western analysis was used to estimate the amount of M-T2 protein secreted from vMyxlac and VV-MT2-infected cells, probing with a 1:5000 dilution of rabbit anti-M-T2 antiserum followed by a 1:5000 dilution of horseradish peroxidase-conjugated goat anti-rabbit IgG antibody (Bio-Rad). The intensities of the bands visualized were measured by scanning using a Joyce Loebel Chromoscan 3 densitometer. The results of four separate Western blots were averaged to determine the amount of M-T2 protein present in supernatants, using various titrations of purified M-T2 protein as the standard.

Co-immunoprecipitation of M-T2 and Rabbit TNF α —To detect M-T2 and rabbit TNF α proteins secreted from recombinant vaccinia virus-infected cells, confluent BGMK cell monolayers in six-well dishes were adsorbed with virus for 1 h at a multiplicity of infection of 10. Next, Dulbecco's modified Eagle's medium, 10% newborn calf serum was added, and the infection was allowed to proceed at 37 °C for 4 h. Cells were washed with PBS and incubated 16 h in 0.5 ml of serum-free, Met-free, Cys-free Dulbecco's modified Eagle's medium containing 150 μ Ci of ³⁵S Express protein label (³⁵S]Met/Cys mixture, DuPont NEN), after which supernatants were collected. 100- μ l supernatants from VV-MT2, VV-T2RaTNF, or VV-601-infected cells were coincubated for 1 h at 4 °C, after which 1 μ g of purified goat anti-rabbit TNF- α antibody (PharMingen) or a 1:200 dilution of rabbit anti-T2 antiserum was added and the mixture was incubated for 1 h further at 4 °C. Next, 30 μ l of protein A beads (10% (v/v) in Nonidet P-40 lysis buffer, 150 mM NaCl, 1.0% Nonidet P-40, 50 mM Tris-Cl, pH 8.0) was added, and the antibody-antigen reaction was incubated 1 h further at 4 °C. The beads were collected by centrifugation at 10,000 \times g for 1 min at 4 °C, and the immune complexes were washed three times with lysis buffer, resuspended in 50 μ l of Laemmli sample buffer, and resolved by SDS-polyacrylamide gel electrophoresis (SDS-PAGE). The gel was dried onto Whatman 3MM chromatography paper and analyzed by autoradiography. Alternatively, 25 ng of purified T2 protein was incubated with 100 μ l of ³⁵S-Met/Cys-labeled supernatant from VV-T2RaTNF-infected cells, and coimmunoprecipitations were performed as above using a 1:200 dilution of rabbit anti-M-T2 antiserum.

Gel Filtration Chromatography of Purified Myxoma T2 Protein—A Superdex 200 gel filtration column (Pharmacia) was calibrated using thyroglobulin, ferritin, catalase, aldolase, and bovine serum albumin (Pharmacia) as size standards. Purified T2 protein was loaded onto the calibrated Sephadex 200 gel filtration column equilibrated with PBS, and fractions were collected. Fractions containing protein were resolved by SDS-PAGE under reducing (50 mM Tris-Cl, pH 6.8, 100 mM dithiothreitol, 2% SDS, 0.1% bromophenol blue, 10% glycerol sample loading buffer) or nonreducing conditions (50 mM Tris-Cl, pH 6.8, 2% SDS, 0.1% bromophenol blue, 10% glycerol sample loading buffer), transferred to nitrocellulose, and probed with a 1:5000 dilution of rabbit anti-M-T2 antisera as described (18).

Sedimentation Equilibrium Analysis—Sedimentation equilibrium studies were performed on a Beckman Spinco model E analytical ultracentrifuge using absorbance optics. The run was performed at 8000 rpm in PBS at 20 °C. The molecular weight (M) was calculated using the equation,

$$M = \frac{2RT}{(1 - \bar{v}\rho)\omega^2} \left[\frac{d(\ln C)}{dr^2} \right] \quad (\text{Eq. 1})$$

where R is the universal gas constant, T is the temperature in Kelvin, \bar{v} is the partial specific volume, ρ is the solvent density, ω is the angular velocity, and $d(\ln C)/dr^2$ is the slope from the plot in Fig. 4. Based on the amino acid composition of M-T2 protein, \bar{v} was calculated to be 0.69. As M-T2 is glycosylated, \bar{v} for the glycoprotein was calculated to be 0.66 using the formula $(M_1 \bar{v}_1 + M_2 \bar{v}_2)/(M_1 + M_2)$, where M_1 , \bar{v}_1 , and M_2 , \bar{v}_2 are the masses and partial specific volume of the protein and the sugar component, respectively.

Solid Phase M-T2 Binding Assay—Purified rabbit TNF α , human TNF α (Quality Controlled Biochemicals), and mouse TNF α (PharMin-

gen) were labeled with Na¹²⁵I (DuPont NEN) to a specific activity of 10⁵ Ci/mole using lactoperoxidase and hydrogen peroxide according to standard procedures (42). Falcon 96-well immunoplates were coated with 100 ng of purified M-T2 protein in 50 µl of PBS, overnight at 4 °C. Wells were blocked with 5% skim milk powder in PBS for 2 h at room temperature, followed by binding of ¹²⁵I-labeled TNFα in 50 µl of blocking buffer for 2 h. Wells were washed three times with PBS, removed, and counted on a Beckman Gamma 5500 radiation counter. To determine the specific binding of M-T2 to TNFα, nonspecific binding in the presence of a 100-fold excess of cold TNFα was subtracted from total binding, and such nonspecific binding routinely represented less than 5% of total binding. All assays were performed in triplicate, and binding of ¹²⁵I-labeled TNFα to myxoma T2 was analyzed by the method of Scatchard (43).

M-T2 Inhibition of Binding of ¹²⁵I-Labeled Rabbit TNFα to RK-13 and RL-5 Cells.—To measure specific binding of ¹²⁵I-labeled rabbit TNFα to RL-5 (rabbit T cell lymphoma) cells, 2 × 10⁶ cells were seeded in microcentrifuge tubes in 100 µl of RPMI medium supplemented with 10% fetal bovine serum, 500 pm ¹²⁵I-labeled rabbit TNFα in the presence or absence of a 100-fold excess of cold TNFα, for 1 h at 4 °C. The cell suspension was then layered over 250 µl of transport oil (15% paraffin oil, 85% silicon 550 oil, specific gravity 1.032 g/ml) in microcentrifuge tubes; the cells were pelleted through the oil by centrifugation at 10,000 × g for 1 min; and the oil and cell pellet were washed three times with water. The cell pellet was resuspended in 0.5% SDS, and the radioactivity present in the cell pellet was measured on a Beckman 5500 γ counter. VV-601 and VV-MT2 supernatants were prepared as described above. To test the ability of M-T2 protein to inhibit binding, 2 × 10⁶ cells were incubated with 500 pm ¹²⁵I-labeled rabbit TNFα and 200 nm purified M-T2 protein or 10% (v/v) VV-601 supernatant or VV-MT2 supernatant containing 50 nm M-T2 protein and processed as described above. All assays were performed in triplicate.

To measure TNF-binding to RK-13 (rabbit fibroblast) cells, 1 × 10⁶ RK-13 cells seeded in six-well dishes were incubated in 200 µl of Dulbecco's modified Eagle's medium supplemented with 10% newborn calf serum. ¹²⁵I-Labeled rabbit TNFα was added to a concentration of 500 pm, in the presence or absence of a 100-fold excess of cold TNF to measure specific binding, or in the presence of 20 nm purified M-T2 protein, and cells were incubated 1 h at 4 °C with gentle agitation. Cells were then washed three times with PBS and resuspended in 200 µl of 0.5% SDS, and the radioactivity remaining in the sample was measured on a Beckman γ counter. All assays were performed in triplicate.

M-T2 Inhibition of TNFα-induced Cytolysis.—The ability of purified myxoma T2 protein to protect rabbit or mouse cells from TNFα-induced cytolysis was measured as described previously (18) except that for RK-13 cells viability was measured by crystal violet staining as described (44). TNFα (rabbit, mouse, human) was used at concentrations for which the cell death end point value was greater than 95% for L929-8 cells and greater than 65% for RK-13 cells. Results are expressed as the percentage of viable cells compared with untreated control cells, the mean of quadruplicate samples calculated by the following formula: ((OD experimental – OD maximum killing)/OD maximum viability – OD maximum killing) × 100, where OD represents optical density. When protection was expressed as an increase in percentage of viability (% viability), the formula (% viability experimental – % viability in the absence of M-T2) was used. In calculating M-T2:TNFα ratios, molarities were calculated for the M-T2 monomer and TNFα trimer unless stated otherwise.

RESULTS

Purification of Myxoma T2 Protein and Rabbit TNFα.—Recombinant vaccinia viruses were engineered to express myxoma T2 protein (VV-MT2) and rabbit TNFα (VV-RaTNF and VV-T2RaTNF) in order to obtain enough protein for binding studies (diagrammed in Fig. 1A). Previously, the complete sequence for the rabbit TNFα cDNA, including the 79-amino acid leader, was placed under the control of the synthetic late promoter in the recombinant virus VV-RaTNF (18). However, TNFα was not efficiently expressed as a secreted ligand from cells infected with VV-RaTNF, so instead the recombinant vaccinia virus VV-T2RaTNF was constructed in which the presequence N-terminal to the mature rabbit TNFα was excised and replaced with the 16-amino acid leader sequence of myxoma T2 protein. Pro-myxoma T2 protein was found by N-terminal se-

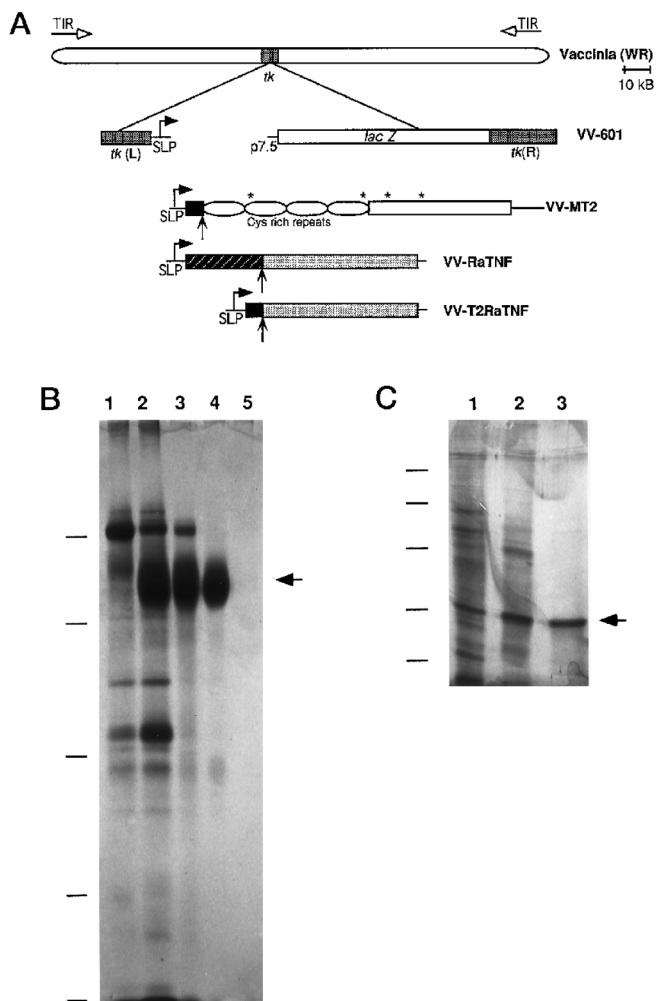


FIG. 1. Structure of recombinant vaccinia viruses expressing M-T2 and rabbit TNFα and purification of MT2 and rabbit TNFα proteins. *A*, structure of VV-601, VV-MT2, VV-RaTNF, and VV-T2RaTNF in which M-T2 sequence, the entire rabbit TNFα coding sequence, or the MT2 leader sequence/mature rabbit TNFα coding sequence was placed under the control of the vaccinia synthetic late promoter (*SLP*) and inserted together with *E. coli* *lacZ* into the *tk* locus of vaccinia-WR. Asterisks indicate predicted *N*-linked glycosylation sites, oval boxes designate the four cysteine-rich repeats of M-T2, arrowheads designate predicted N-terminal cleavage sites, and *TIR* designates the terminal inverted repeats. *B*, purification of M-T2 displaying proteins present in crude supernatants from VV-601 (*lane 1*) or VV-MT2-infected cells (*lane 2*), purity of MT2 after the first anion exchange chromatography, pH 7.5 (*lane 3*), followed by a second anion exchange chromatography, pH 6.4 (*lane 4*), and corresponding fraction from control VV-601 supernatants (*lane 5*). *C*, purification of secreted rabbit TNFα from crude supernatants from VV-T2RaTNF-infected cells (*lane 1*) and purity of rabbit TNFα after the first anion exchange chromatography, pH 7.5 (*lane 2*), followed by a second anion exchange chromatography, pH 6.4 (*lane 3*). Size standards of 66.2, 45, 31, 21.5, and 14.4 kDa are marked on panels *B* and *C*.

quencing to be cleaved at its predicted signal cleavage site between Gly-16 and Gly-17. The biologically active rabbit TNFα secreted from VV-T2RaTNF-infected cells has a molecular mass on SDS-polyacrylamide gels identical to the 18-kDa reported molecular mass of rabbit TNFα (45) (Fig. 1C).

Both myxoma T2 protein and rabbit TNFα were purified from supernatants from virally infected BGMK cells by two rounds of anion-exchange Mono-Q chromatography at pH 7.5 and 6.4. Fig. 1B displays proteins present in crude supernatants from cells infected with vector control vaccinia virus, VV-601 (*lane 1*), and cells infected with VV-MT2 (*lane 2*). At pH 7.5, M-T2 protein eluted from the column at 150–280 mM NaCl

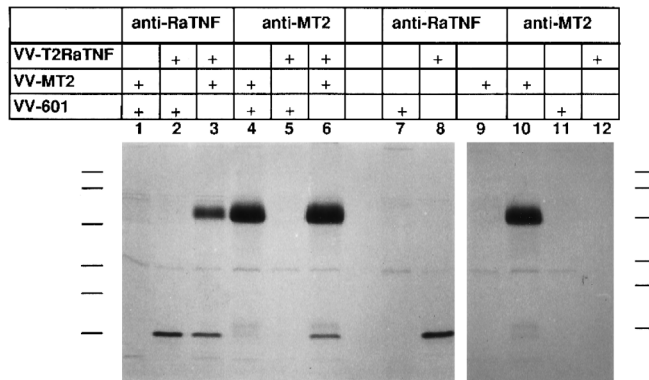


Fig. 2. Co-immunoprecipitations of MT2 and rabbit TNF α . ^{35}S -Labeled proteins from VV-T2RaTNF-infected cells (lanes 2, 3, 5, 6, 8, and 10), VV-MT2-infected cells (lanes 1, 3, 4, 6, 9, and 10), or control VV-601-infected cells (lanes 1, 2, 4, 5, 7, and 11) were combined in pairs (lanes 1–6), or singly (lanes 7–12), and immunoprecipitated with anti-rabbit TNF α antibody (lanes 1–3 and lanes 7–9) or polyclonal rabbit anti-MT2 antisera (lanes 4–6 and lanes 10–12) as described under “Materials and Methods” and analyzed by SDS-PAGE and autoradiography. Size standards of 112, 84, 53.2, 34.9, 28.7, and 20.5 kDa are indicated.

(lane 3). When re-applied to the anion exchange column at pH 6.4, a single protein band was observed on silver-stained SDS-PAGE gels in fractions collected at 100–150 mM NaCl, with no protein bands seen from supernatants from vector control virus, VV601, processed in identical fashion (Fig. 1B, lanes 4 and 5, respectively).

The purification of rabbit TNF α is illustrated in Fig. 1C, starting from supernatants of VV-T2RaTNF-infected monolayers (lane 1). At pH 7.5, rabbit TNF α eluted from the Mono-Q column at 300–340 mM NaCl (Fig. 1C, lane 2). TNF-containing fractions were pooled and re-applied to the Mono-Q column at pH 6.4, and rabbit TNF α eluted at 260–275 mM NaCl as a single 18-kDa species when visualized on silver-stained gels (Fig. 1C, lane 3).

The amount of M-T2 protein secreted into supernatants from BGMK cells infected with either VV-MT2 or vMyxlac virus was quantitated from densitometric scans of Western blots, using various titrations of purified M-T2 protein as standards. As expected, the amount of M-T2 protein secreted from VV-MT2-infected cells was significantly higher than from myxoma-infected cells: $(1.0 \pm 0.4) \times 10^8$ molecules/24 h of M-T2 secreted per VV-MT2-infected cell compared with $(2.8 \pm 0.5) \times 10^6$ molecules/24 h of M-T2 secreted per vMyxlac infected cell. In VV-MT2, the M-T2 gene is under the control of a very strong synthetic late promoter (40), which accounts for the enhanced expression compared with the standard (early) promoter in the parental myxoma virus.

Myxoma T2 Protein Specifically Complexes with Rabbit TNF α —To determine whether M-T2 protein and rabbit TNF α physically associate, immunoprecipitation experiments were performed. M-T2 polyclonal antibody correctly immunoprecipitates native M-T2 protein, with an apparent molecular mass of 60 kDa, from supernatants from ^{35}S -Met/Cys-labeled VV-MT2 infected cells (Fig. 2, lanes 4 and 10) but not from control VV-601- or VV-T2RaTNF-infected cells (Fig. 2, lanes 5, 11, and 12). Similarly, anti-rabbit TNF α antibody only immunoprecipitates rabbit TNF α , an 18-kDa protein from supernatants from VV-T2RaTNF-infected cells (lanes 2 and 8) but not from VV-601- or VV-MT2-infected cells (lanes 1, 7, and 9). When supernatants from VV-601- or VV-MT2-infected cells were co-incubated with supernatants from VV-T2RaTNF-infected cells for 1 h and then immunoprecipitated with anti-rabbit TNF α antibody, radiolabeled proteins of sizes identical to myxoma T2

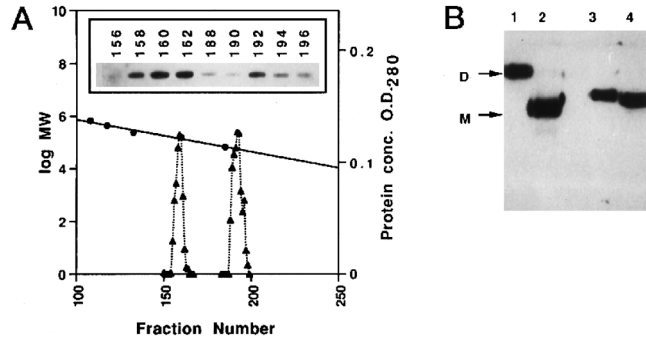


Fig. 3. Native size of M-T2 protein. *A*, elution profile of purified M-T2 protein fractionated by Superdex 200 gel filtration chromatography, showing protein concentration, A_{280} (triangles) as a function of fraction number. The inset shows a Western blot of a reducing SDS-PAGE gel testing various fractions, probed with a rabbit anti-MT2 antiserum. Elution of size standards bovine serum albumin (67 kDa), aldolase (158 kDa), catalase (232 kDa), ferritin (440 kDa), and thyroglobulin (669 kDa) (circles) is shown as a function of the log molecular weight. *B*, Western blot of protein present in fraction 160 (lanes 1 and 3) and fraction 192 (lanes 2 and 4) run under nonreducing (lanes 1 and 2) and reducing (lanes 3 and 4) conditions and probed with rabbit anti-MT2 antisera as outlined under “Materials and Methods.” *D*, dimer; *M*, monomer.

protein and rabbit TNF α were co-precipitated in VV-MT2/VV-T2RaTNF mixtures (Fig. 2, lane 3). Similarly, anti-myxoma T2 antisera was able to co-precipitate both rabbit TNF α and myxoma T2 proteins from mixtures of VV-MT2/VV-T2RaTNF (lane 6). Thus, both polyclonal antisera against myxoma T2 protein and anti-rabbit TNF α antibody were each able to coimmunoprecipitate the complex between rabbit TNF α and myxoma T2 protein. In contrast, anti-myxoma T2 antisera was unable to co-immunoprecipitate ^{35}S -radiolabeled myxoma T2 and ^{125}I -radiolabeled mouse TNF α (data not shown).

Native Size of M-T2 Protein Secreted from Virus-infected Cells—Purified T2 protein was fractionated by Superdex 200 gel filtration chromatography to determine whether it is expressed as a monomer or oligomer. N-terminal sequencing had shown this to be a pure preparation of M-T2. However, as shown in Fig. 3A, M-T2 protein eluted from the column as two distinct peaks, estimated to be 140–156 kDa and 56–65 kDa in size, based on size standards of a variety of monomeric proteins. When samples from these two peaks were analyzed by SDS-PAGE under reducing conditions and probed by Western blotting, anti-M-T2 antisera recognized only a single 55–60-kDa protein band in fractions from both peaks (Fig. 3A, inset), indicating that the first peak to elute from the Superdex column is most likely an oligomeric form of the second peak. When analyzed under nonreducing conditions, the first eluted M-T2 peak electrophoresed as a single 87–90-kDa band on SDS-polyacrylamide gels (Fig. 3B, lane 1), whereas the second M-T2 peak eluted from the Superdex column electrophoresed as a single 55–59-kDa species (lane 2). However, both M-T2 species co-migrated at approximately 60 kDa when the samples were reduced with dithiothreitol prior to electrophoresis, suggesting that the two M-T2 peaks detected by Superdex chromatography (Fig. 3A) are the monomeric and disulfide-linked dimeric forms of the same M-T2 protein. To confirm this result and to resolve the discrepancies in the apparent molecular mass of M-T2 protein determined by SDS-PAGE and gel filtration chromatography, the oligomeric protein from the first Superdex 200 M-T2 peak was examined by mass spectrometry and ultracentrifugation studies. When analyzed by mass spectrometry, a mass of 80.9 kDa was calculated for the larger species, confirming that it is in fact a dimer of a 40.5-kDa species. Moreover, by ultracentrifugation sedimentation analysis, the plot of $\ln C$ versus r^2 yielded a straight line, indicating that this larger

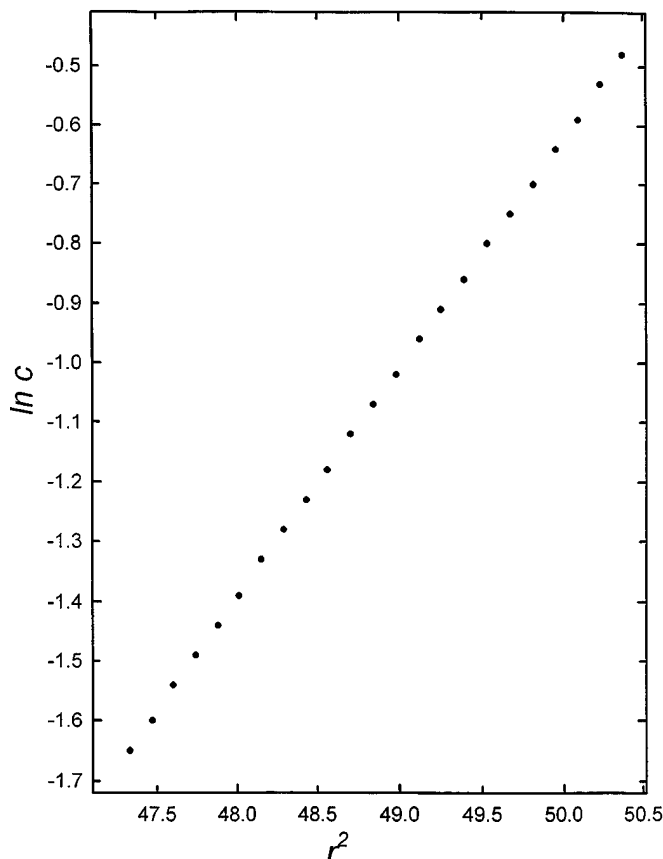


FIG. 4. Ultracentrifugation analysis of M-T2 protein. Shown is the analysis of the sedimentation equilibrium run performed as described under "Materials and Methods," showing the plot of $\ln C$ versus r^2 , where C is the concentration in absorbance units at 280 nm and r is the distance from the axis of rotation (cm). The molecular mass of ~ 79 kDa was calculated from the slope using the equation given under "Materials and Methods."

M-T2 peak from the Superdex 200 column is a single species with a calculated molecular mass of approximately 79 kDa (Fig. 4).

Scatchard Analysis of M-T2 Binding to TNF α —To quantitate the affinity of M-T2 protein for rabbit TNF α , solid phase binding assays were performed, followed by Scatchard analysis. Experiments with M-T2 protein containing both monomeric and dimeric forms yielded a single slope (not shown), indicative of a single affinity binding site, but to substantiate this interpretation, binding analysis was carried out on the purified M-T2 monomer and dimer individually. The binding of ^{125}I -radiolabeled rabbit TNF α with both dimeric and monomeric M-T2 protein, separated by gel filtration chromatography (Fig. 3A), was therefore examined using various concentrations of labeled TNF α either in the presence or absence of excess unlabeled ligand. The specific binding of rabbit TNF α increased with increasing concentration of labeled ligand and reached saturation at 500 pm for both dimeric and monomeric M-T2 (Fig. 5A and B). For both forms of M-T2 the Scatchard plot of the binding data was consistent with a single class of high affinity binding sites with similar affinities, a calculated K_d of 195 pm with a correlation coefficient of -0.95 for dimeric M-T2 (Fig. 5A), and a K_d of 170 pm with a correlation coefficient of -0.96 for monomeric M-T2 (Fig. 5B).

Saturable binding was also observed between M-T2 protein, containing both monomeric and dimeric species, and ^{125}I -radiolabeled mouse TNF α but only at a higher concentration in the nm range (Fig. 5C), while no binding at all was observed with radiolabeled human TNF α (Fig. 5D). The affinity of myxoma T2 and mouse TNF α was an order of magnitude lower than the affinity of M-T2 with

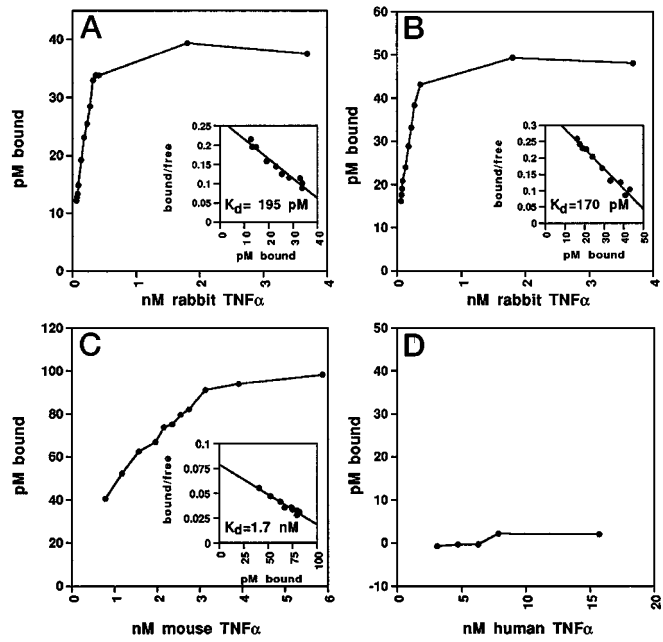


FIG. 5. Solid phase equilibrium binding analysis of rabbit, mouse, and human ^{125}I -labeled TNF α to M-T2 protein. Shown are solid phase analysis of dimeric (A) and monomeric (B) MT2 protein with ^{125}I -labeled rabbit TNF α and Scatchard analysis (insets) of the binding curve of ^{125}I -labeled rabbit TNF α and MT2, as outlined under "Materials and Methods". C, solid phase analysis of MT2 protein with ^{125}I -labeled mouse TNF α , and Scatchard analysis (inset) of the binding curve of ^{125}I -labeled mouse TNF α and MT2. D, solid phase analysis of MT2 protein with ^{125}I -labeled human TNF α .

rabbit TNF α , and the K_d was calculated to be 1.7 nm with a correlation coefficient on the Scatchard plot of -0.98 . Thus, the biological specificity of M-T2 for rabbit TNF α (18) is consistent with this physical binding data.

Rabbit TNF receptors have not yet been cloned or characterized. Attempts to determine the K_d of cognate rabbit TNF receptors with rabbit TNF α were unsuccessful because of the low number of TNF receptors present on all rabbit cell lines screened. Instead, we tested to see whether M-T2 protein can inhibit the binding of ^{125}I -labeled rabbit TNF α to cellular receptors on two rabbit cell lines that exhibited some TNF binding. Rabbit RL-5 cells, a CD4 $^+$ -T cell lymphoma cell line, and RK-13 cells, a fibroblast kidney line, were incubated with 500 pm ^{125}I -rabbit TNF α in the presence or absence of a 100-fold excess of cold TNF to determine specific binding. As shown in Fig. 6, a 400-fold molar ratio excess of purified M-T2 protein, 200 nm, was able to effectively block specific binding of rabbit TNF α to both RL-5 cells (lane 2) and RK-13 cells (lane 6). Similarly, even crude supernatant from VV-MT2-infected BGMK cells, containing approximately 50 nm M-T2 protein, was also able to inhibit binding of radiolabeled rabbit TNF α to RL-5 cells (lane 3), whereas control supernatant from VV-601-infected cells (lane 4) had no effect. Thus, we conclude that M-T2 protein as secreted from infected cells actually blocks the binding of rabbit TNF α to the cell surface of rabbit fibroblasts and lymphocytes.

Myxoma T2 Specifically Inhibits Rabbit but Not Mouse TNF α —Previously we had shown that myxoma T2 protein present in crude supernatants from VV-MT2-infected cells was able to inhibit the cytolytic activities of rabbit TNF α on mouse L929-8 cells but not the mouse or human ligands (18). Since myxoma T2 was found by Scatchard analysis to bind both rabbit and mouse TNF α , albeit with different affinities (Fig. 5), anion exchange chromatography-purified myxoma T2 protein, containing both monomers and dimers, was tested for its abil-

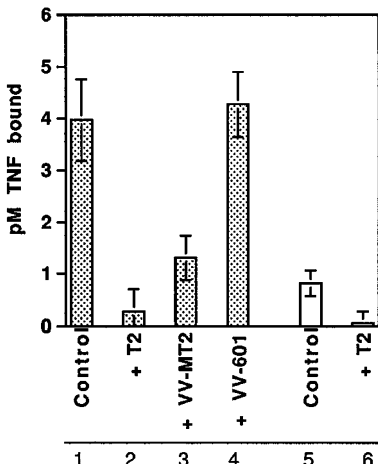


FIG. 6. M-T2 inhibition of the binding of rabbit TNF α to rabbit membrane TNFRs. 2×10^6 RL-5 cells (speckled box) or 1×10^6 RK-13 cells (open box) were incubated with 500 pm 125 I-labeled rabbit TNF α in the presence and absence of a 100-fold excess of cold TNF α to determine ligand-specific binding to the cell surface. 200 nm purified M-T2 protein, or 10% (v/v) supernatant from VV-601-infected or VV-MT2-infected cells (containing approximately 50 nm MT2 protein) was added as indicated, as outlined under “Materials and Methods.” Standard deviations of triplicate assays are shown.

ity to protect the TNF-hypersensitive mouse L929-8 cell line from lysis by mouse and rabbit TNF α . Viability of actinomycin-treated L929-8 cells incubated for 24 h with various concentrations of mouse TNF α was examined in the presence of increasing amounts of myxoma T2 protein, and the increase in cell viability with M-T2 present was plotted against the molar ratio of myxoma T2:mouse TNF α . As shown in Fig. 7A, myxoma T2 protein did not engender enhanced viability of L929-8 cells even at M-T2:mouse TNF α ratios approaching 50,000:1. However, M-T2 protein, containing a mixture of both monomeric and dimeric forms, was able to protect L929-8 cells from lysis by rabbit TNF α at ratios of 10:1 for M-T2:rabbit TNF α (Fig. 7B) with complete protection against rabbit TNF α seen at ratios of 400:1.

Although rabbit TNF α is active on mouse cells, it is of relevance to assess the more biologically relevant interaction with rabbit cells. The ability of myxoma T2 protein to protect rabbit RK-13 cells from lysis by rabbit TNF α was also tested. Actinomycin D-sensitized RK-13 cells are not as susceptible to TNF cytotoxicity as are L929-8 cells and evidence a maximal loss of viability down to 30% of untreated cultures even at the highest rabbit TNF α concentrations tested. When exposed to rabbit TNF α concentrations at which cytotoxicity was maximal, myxoma T2 protein was able to effectively protect RK-13 cells against lysis by rabbit TNF α , with complete protection observed at M-T2:rabbit TNF α monomer molar ratios of 50:1. (Fig. 7C).

Dimeric M-T2 Protein Is Much More Effective than the Monomer at Inhibiting the Cytolytic Activity of Rabbit TNF α —To determine whether the monomeric and dimeric forms of M-T2 are comparably active at inhibiting the biological activities of rabbit TNF α , actinomycin-sensitized L929-8 cells were incubated with increasing amounts of rabbit TNF α in the presence of 5 nm dimeric T2 or 10 nm monomeric T2. As shown in Fig. 8A, a 5-fold molar excess of dimeric M-T2 protein (solid squares) can protect against TNF α -induced lysis, with complete protection detected by 50-fold excess. However, 10 nm monomeric M-T2 (triangles) was completely unable to protect L929-8 from lysis by rabbit TNF α compared with controls (circles). Only when present at much higher concentrations was monomeric M-T2 protein able to protect against TNF α -induced cytotoxicity, in that 80% protection was observed at a 2000-fold molar excess of monomeric M-T2 protein (Fig. 8B, triangles). Interestingly,

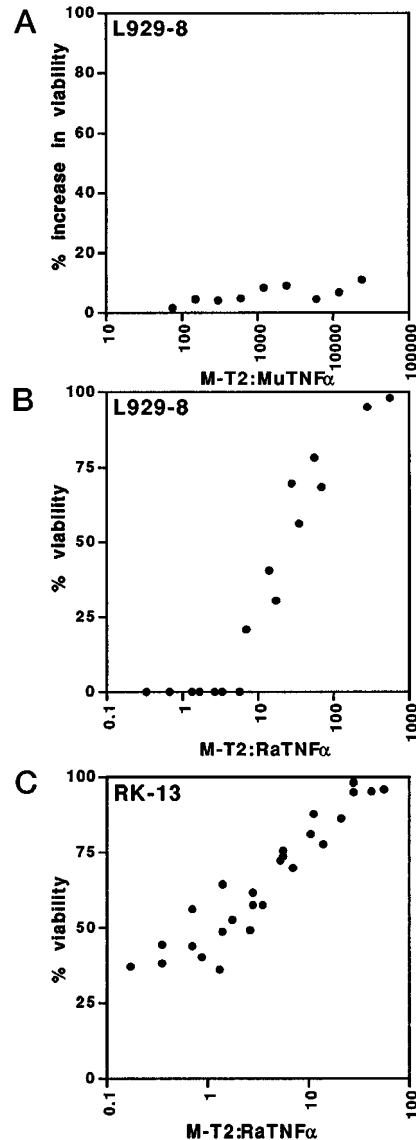


FIG. 7. M-T2 protects against cytolysis by rabbit but not mouse TNF α . Actinomycin D-sensitized L929-8 cells (A and B) or RK-13 cells (C) were incubated at varying molar ratios of M-T2 protein and mouse TNF α (A) or rabbit TNF α (B and C) as described under “Materials and Methods” and the percentage increase in cell viability (A) or percentage of viability of cells (B and C) determined by neutral red uptake (A and B) or crystal violet staining (C). A monomeric size of 40 kDa was calculated for M-T2, while the trimeric size of 54 kDa for rabbit TNF α and 51 kDa for mouse TNF α was used. Points represent the mean of quadruplicate determinations.

comparable levels of rabbit TNF α were able to co-immunoprecipitate with both the M-T2 monomer and dimer. When 35 S-Met/Cys-labeled rabbit TNF α was co-incubated with either monomeric or dimeric M-T2 protein and then immunoprecipitated with anti-M-T2 antisera (Fig. 8C) both monomeric and dimeric M-T2 protein co-immunoprecipitated similar amounts of rabbit TNF α (lanes 3 and 4), indicating that both forms of M-T2 protein form stable complexes with rabbit TNF α . We conclude that dimeric M-T2, with two ligand binding sites, can likely occlude two of the three TNF α receptor binding domains present in a TNF α trimer and is therefore a much more effective inhibitor of TNF α than is monomeric M-T2.

DISCUSSION

Myxoma virus, a member of the poxvirus family of viruses, encodes a wide spectrum of immunomodulatory proteins, including several secreted homologs of cytokine receptors (46,

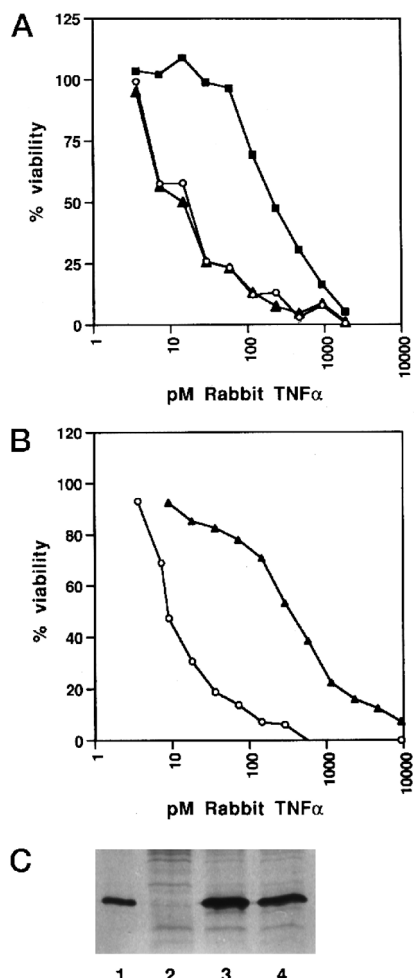


FIG. 8. Protection against TNF- α induced cytotoxicity by monomeric and dimeric M-T2 protein. *A*, actinomycin D-sensitized L929-8 cells were incubated with increasing amounts of rabbit TNF- α alone (circles) or in the presence of 5 nM dimeric M-T2 (squares) or 10 nM monomeric M-T2 (triangles), and cell viability was determined by neutral red uptake as outlined under "Materials and Methods." Each point represents the mean of quadruplicate determinations. *B*, actinomycin D-sensitized L929-8 cells were incubated with increasing amounts of rabbit TNF- α alone (circles) or in the presence of 200 nM monomeric M-T2 (triangles). *C*, 35 S-labeled supernatants from VV-T2RaTNF-infected cells were incubated with no MT2 (lanes 1 and 2) or 25 ng of dimeric M-T2 (lane 3) or monomeric M-T2 (lane 4), immunoprecipitated with rabbit anti-MT2 antisera (lanes 2-4) or anti-rabbit TNF- α antibody (lane 1), and analyzed by SDS-PAGE as outlined under "Materials and Methods." The autoradiogram showing immunoprecipitated rabbit TNF- α is displayed.

47). M-T2 protein, which is encoded by two copies of the T2 gene, possesses homology to the extracellular ligand binding domains of the TNFRs and presumably acts as a TNF antagonist, binding and sequestering host TNF, thus preventing this ligand from participating in the local antiviral response (12). Previously we have shown that M-T2 protein inhibits the cytolytic activity of rabbit TNF- α on mouse L929-8 cells, but not mouse or human TNF- α (18). Here we show that M-T2 and rabbit TNF- α form stable inhibitory complexes and that the dimeric form of M-T2 is the superior inhibitor of TNF- α biological activity.

Biochemical characterization of M-T2 protein revealed that it is secreted from virus-infected cells as both a 40-kDa monomer and an 80-kDa disulfide-linked dimer. Because of discrepancies in the apparent molecular weights between SDS-PAGE and gel filtration analysis, we used mass spectrometry and ultracentrifugation sedimentation equilibrium techniques to

confirm the size and oligomeric status of M-T2. M-T2 protein was detected as both a monomer, approximately 40 kDa in size, and an 80.9-kDa dimer, as determined by mass spectroscopy. Moreover, sedimentation equilibrium analysis of the dimer indicated that it was a single stable species, of approximately 79 kDa. The calculated molecular mass from amino acid composition of unmodified, monomeric, secreted M-T2 is predicted to be 33 kDa. The difference between the theoretical and observed molecular masses can be accounted for by *N*-linked glycosylation at one or more of the four predicted glycosylation sites on the M-T2 protein.²

Both the monomeric and dimeric forms of M-T2 protein form stable complexes with rabbit TNF- α with similar binding affinities. High affinity binding with K_d values of 170 and 195 pm were observed between rabbit TNF- α and monomeric and dimeric M-T2, respectively, by solid phase binding and Scatchard analysis. Because of the low number of TNFRs present on rabbit cell lines tested, we were unable to accurately quantitate the affinity of rabbit TNF- α for rabbit cell surface TNFRs, but reported K_d values for the binding of human and mouse TNF- α to the p75 TNFR range from 50 to 500 pm (32, 48-50), whereas the p55 TNFR displays a somewhat lower affinity with reported K_d values ranging from 130 to 2300 pm (50-52). The calculated K_d for myxoma T2 protein with rabbit TNF- α thus compares favorably with the K_d values determined for the human and mouse TNFRs with their cognate TNF- α s.

Soluble TNFRs, consisting of truncated versions of the extracellular ligand binding domains of the p55 and the p75 receptors, bind TNF- α with an affinity comparable with the full-length membrane receptors (48, 51, 53). This is in contrast to many soluble receptors, including the IFN- γ receptor, which often bind their respective ligands with lower affinity than the membrane-bound counterpart (54, 55). The myxoma virus homolog of the IFN- γ receptor (M-T7), proposed to act in an analogous fashion to M-T2, binds rabbit IFN- γ with a K_d of 1.2 nm (5), which is 6-7-fold lower affinity than M-T2 for rabbit TNF- α . However, M-T7 is by far the most abundantly secreted viral protein from myxoma-infected cells (4), with 4×10^7 molecules secreted per infected cell in the first few hours of myxoma infection (5), whereas only 3×10^6 molecules of M-T2 are secreted per infected cell over the course of a single infection cycle. Moreover a wide variety in the number of TNF receptors present on various cell types has been reported, ranging from 100 to 10,000 copies (32, 56, 57), which may be accounted for by a low, constitutive expression of p55 TNFR (1000 copies/cell (57)) and an inducible level of p75 TNFR expression (32, 57). It is the p55 TNFR which is believed to signal the vast majority of the pathogen response activities of TNF (33, 34) including cytotoxicity (35, 58) and antiviral activity (59). Thus, we presume that M-T2 must block ligand interaction with the presumptive rabbit version of the p55 TNFR to inhibit the direct cytolytic or antiviral activities of TNF- α . The level of M-T2 protein secreted from infected cells is still in vast excess over the estimated number of p55 TNFRs present on TNF-responsive cells, and levels of M-T2 secreted by myxoma virus should therefore be sufficient to inhibit TNF- α within the microenvironment of virus-infected tissues.

Full-length p55 receptor has an equivalent affinity for both TNF- α and TNF- β , while the soluble version of the same receptor displays a 50-60-fold lower affinity for TNF- β (53, 60). A comparison of M-T2 affinity for rabbit TNF- α and TNF- β would indicate whether TNF- β is also a candidate for M-T2 inhibitory action as well. However, although the rabbit TNF gene locus has been sequenced, and the amino acid sequence of rabbit

TNF β has been deduced from the genomic sequence (61), all our attempts at isolating rabbit TNF β cDNA using this sequence were unsuccessful; thus, we cannot at this point comment on whether rabbit TNF β is a biologically relevant target for M-T2 in addition to rabbit TNF α .

Although solid phase saturable binding between mouse TNF α and myxoma T2 protein was measured (K_d of 1.7 nM), we were unable to co-immunoprecipitate M-T2 protein complexed with mouse TNF α (data not shown). Moreover, purified myxoma T2 protein was unable to protect mouse L929-8 cells from lysis by mouse TNF even at M-T2:TNF α molar ratios of 50,000:1, confirming our earlier observations on the species specificity of M-T2 (18) and further reinforcing the idea that binding and inhibition are not synonymous for this class of viral cytokine inhibitors.

On the other hand, purified M-T2 protein was able to effectively protect mouse and rabbit cells from lysis by rabbit TNF α , with 50% protection observed at 50-fold molar excess of M-T2 protein and complete protection observed at 300-fold molar excess of M-T2. M-T2 protein was even more effective at protecting rabbit RK-13 cells from lysis by rabbit TNF α in that a 50% inhibition of TNF cytotoxicity was observed at only a 10-fold molar excess of M-T2, and complete protection was seen at 50-fold excess. Thus, M-T2 protein is able to prevent rabbit TNF α signaling not only through heterologous mouse TNFRs but also to the homologous rabbit TNFRs. One might predict that rabbit TNF receptors would have a higher affinity for rabbit TNF α than do the mouse receptors and that M-T2 protein would be better at competing with mouse TNFRs than rabbit receptors for binding rabbit TNF α . However, it should be cautioned that L929-8 cells were selected for their hypersensitivity to TNF (including the mouse, human, and rabbit ligand), and the increased amounts of M-T2 protein required for protection may simply reflect a heightened capacity of L929-8 cells to effect a TNF signaling cascade with relatively fewer molecules of TNF binding to surface receptors.

A 10–500-fold molar excess of human p55 soluble TNFR is required to inhibit the cytolytic activity of human TNF α on various cell lines (51, 53, 62, 63), which compares favorably with the ratios of M-T2 required to inhibit rabbit TNF α . In comparing the ability of the human soluble p55 and p75 receptors to inhibit the cytolytic effects of human TNF α on L929-8 cells, Hale *et al.* (62) found that the soluble p55 receptor was a 10-fold more potent inhibitor than the soluble p75 receptor. Moreover, the soluble p55 receptor was 100-fold more effective than soluble p75 receptor at blocking binding of TNF α to U-937 cells (64). The kinetics of association and dissociation of TNF with the p75 TNFR is much more rapid than with the p55 TNFR (65), which may account for its reduced effectiveness as a TNF α inhibitor. Although M-T2 and the related S-T2 protein from Shope fibroma virus show greater sequence similarity with the p75 TNFR than the p55 TNFR (66), we show here that M-T2 protein is as potent an inhibitor of TNF cytology as is the soluble p55 TNFR.

According to our model of M-T2 action, M-T2 sequesters TNF α into stable inhibitory complexes and prevents its association with receptors present on the cell surface. However, another possibility is that M-T2 binding of TNF α may not necessarily occlude binding of the TNF α trimer to cellular receptors but may prevent receptor-bound TNF α from signaling, perhaps by preventing the subsequent clustering of membrane TNF receptors. However, we have shown that a 400-fold molar excess of M-T2 was able to effectively block binding of 125 I-labeled rabbit TNF α to both rabbit lymphocytes and fibroblasts to near background levels. At this molar ratio of M-T2:TNF α , RK-13 fibroblast cells show complete protection against

lysis by TNF α , although the same experiment could not be performed with RL-5 lymphocytes because they are not sensitive to TNF cytotoxicity.³ As the protective capabilities of M-T2 correlate with its ability to inhibit binding of TNF α to membrane receptors, we conclude that M-T2 inhibits the cytolytic activities of TNF α by physically preventing TNF α from associating with its cognate TNF membrane receptors.

Although both the monomeric and dimeric species of M-T2 bind rabbit TNF α with similar affinities, the dimeric form of M-T2 was much more effective at inhibiting cytosis of L929-8 cells by rabbit TNF α than the monomeric form. A 25-fold molar excess of dimeric M-T2 protein, compared with a 2000-fold excess of monomeric M-T2 protein, was required to completely inhibit the cytolytic activity of rabbit TNF α on L929-8 cells. Similar observations have been made with monomeric and dimeric forms of the cellular soluble TNFRs. Dimeric soluble TNFRs, consisting of chimeric immunofusion proteins of the extracellular ligand binding domains with human IgG Fc, are much more active at inhibiting the biological activities of TNF α than the corresponding soluble receptors (51, 54, 63, 67–69). Concentrations of dimeric soluble p55 TNFR equimolar to TNF α are sufficient to neutralize the cytolytic activity of TNF α on WEHI-164, SK MEL 109, and KYM-1D4 cells, whereas a 10–1000-fold excess of soluble p55 TNFR monomer was required to achieve similar levels of inhibition (51, 70, 71). Part of the enhanced inhibitory activity of the bivalent immunofusion proteins can be accounted for by their higher affinity for TNF α than the monovalent soluble TNFRs (51, 54, 68), which most likely reflects an increased avidity of the bivalent construct for its ligand. However, the difference between the dimeric constructs and soluble receptors in inhibiting TNF α activity (10–1000-fold) is significantly greater than their differences in binding affinity for TNF α (6–8 fold). Clustering of membrane-bound TNFRs, either by dimerization or trimerization, is believed to be important in establishing a downstream signal (29, 30, 32). Dimerization of erythropoietin/p55 or p75 TNFR chimeras is sufficient to elicit a biological response (72, 73), although receptor dimerization may be less effective at initiating signal transduction cascades than trimerization (32, 73). Dimeric soluble TNFRs could simultaneously block two receptor binding sites on a single TNF α trimer, thus rendering TNF α unable to even dimerize cell surface TNF receptors (67), whereas two soluble TNFRs would have to bind a TNF trimer in order to similarly inactivate it from dimerizing receptors. Dimeric M-T2 protein thus could act in an analogous fashion, by preventing even dimerization of cellular TNFRs, which would account for its 100-fold greater inhibitory activity over that of the monomeric M-T2 protein. Thus, we conclude that poxviruses exploit the greater inhibitory capacity of linked receptor dimers, thus strengthening the concept that the effective blockade of cytokine function can be achieved by sequestering important ligands such as TNF into inhibitory complexes that disallow receptor oligomerization and subsequent intracellular signaling cascades.

Acknowledgments—We thank K. Mossman for helpful discussions on solid phase binding assays, Dr. C. Kay and L. Hicks for contributions toward sedimentation equilibrium, P. Semchuk for help with the mass spectrometry, and R. Maranchuk for excellent technical assistance.

REFERENCES

1. Moss, B. (1990) in *Virology* (Fields, B. N., and Knipe, D. M., eds) pp. 2079–2111, Raven Press, New York
2. McFadden, G. (ed) (1995) *Viroceptors, Virokines and Related Immune Modulators Encoded by DNA Viruses*, R. G. Landes Co., Austin

³ M. Schreiber and G. McFadden, unpublished observations.

3. Smith, G. L. (1994) *Trends Microbiol.* **2**, 80–88
4. Upton, C., Mossman, K., and McFadden, G. (1992) *Science* **258**, 1369–1372
5. Mossman, K., Upton, C., and McFadden, G. (1995) *J. Biol. Chem.* **270**, 3031–3038
6. Alcami, A., and Smith, G. L. (1995) *J. Virol.* **69**, 4633–4639
7. Mossman, K., Upton, C., Buller, R. M. L., and McFadden, G. (1995) *Virology* **208**, 762–769
8. Symons, J., Alcami, A., and Smith, G. L. (1995) *Cell* **81**, 551–560
9. Colamonti, O. R., Domanski, P., Sweitzer, S. M., Larner, A., and Buller, R. M. L. (1995) *J. Biol. Chem.* **270**, 15974–15978
10. Spriggs, M., Hruby, D., Maliszewski, C., Pickup, D., Sims, J., Buller, R. M., and VanSlyke, J. (1992) *Cell* **71**, 145–152
11. Alcami, A., and Smith, G. L. (1992) *Cell* **71**, 153–167
12. Upton, C., Macen, J. L., Schreiber, M., and McFadden, G. (1991) *Virology* **184**, 370–382
13. Hu, F.-Q., Smith, C. A., and Pickup, D. J. (1994) *Virology* **204**, 343–356
14. Alcami, A., and Smith, G. L. (1995) *Immunol. Today* **16**, 474–478
15. Spriggs, M. (1994) *Virus Res.* **33**, 1–10
16. Fenner, F., and Ratcliffe, F. N. (1965) *Myxomatosis*, Cambridge University Press, Cambridge
17. McFadden, G. (1994) in *Encyclopedia of Virology* (Webster, R., and Cranoff, A., eds) pp. 1153–1160, Academic Press, Inc., San Diego
18. Schreiber, M., and McFadden, G. (1994) *Virology* **204**, 692–705
19. Tracey, K. J., and Cerami, A. (1994) *Annu. Rev. Med.* **45**, 491–503
20. Beutler, B. (1991) in *Peptide Growth Factors and their Receptors* (Sporn, M., and Roberts, A., eds) pp. 39–70, Springer-Verlag, New York
21. Wong, G. H. W., and Goeddel (1986) *Nature* **323**, 819–822
22. Aderka, D., Novick, D., Hahn, T., Fischer, D. G., and Wallach, D. (1985) *Cellular Immunology* **92**, 218–225
23. Koff, W. C., and Fann, A. V. (1986) *Lymphokine Res.* **5**, 215–221
24. Lorence, R. M., Rood, P. A., and Kelley, K. W. (1988) *J. Natl. Cancer Inst.* **80**, 1305–1312
25. Lester, S. M., Wold, W. S. M., and Gooding, L. R. (1994) *Semin. Virology* **5**, 431–442
26. Sambhi, S. K., Kohonin-Corish, M. R. J., and Ramshaw, I. A. (1991) *Proc. Natl. Acad. Sci. U. S. A.* **88**, 4025–4029
27. Lidbury, B. A., Ramshaw, I. A., and Sambhi, S. K. (1995) *Cytokine* **7**, 157–164
28. Wold, W. S. M. (1993) *J. Cell. Biochem.* **53**, 329–335
29. Wells, J. A. (1994) *Curr. Opin. Cell Biol.* **6**, 163–173
30. Heldin, C.-H. (1995) *Cell* **80**, 213–223
31. Pfizenmaier, K., Himmeler, A., Schutze, S., Scheurich, P., and Kronke, M. (1992) in *Tumor Necrosis Factors: The Molecules and Their Emerging Role in Medicine* (Beutler, B., ed) pp. 439–472, Raven Press, Ltd., New York
32. Vandenebeele, P., Declercq, W., Beyaert, R., and Fiers, W. (1995) *Trends Cell Biol.* **5**, 392–399
33. Tartaglia, L. A., and Goeddel, D. V. (1992) *Immunol. Today* **13**, 151–153
34. Wiegnmann, K., Schutze, S., Kampen, E., Himmeler, A., Machleidt, T., and Kronke, M. (1992) *J. Biol. Chem.* **267**, 17997–18001
35. Tartaglia, L. A., Rothe, M., Hu, Y.-F., and Goeddel, D. V. (1993) *Cell* **73**, 213–216
36. Armitage, R. (1994) *Curr. Opin. Immunol.* **6**, 407–413
37. Smith, C. A., Farrah, T., and Goodwin, R. (1994) *Cell* **76**, 959–962
38. Macen, J. L., Upton, C., Nation, N., and McFadden, G. (1993) *Virology* **195**, 348–363
39. Opgenorth, A., Graham, K., Nation, N., Strayer, D., and McFadden, G. (1992) *J. Virol.* **66**, 4720–4731
40. Davison, A. J., and Moss, B. (1990) *Nucleic Acids Res.* **18**, 4285–4286
41. Garfin, D. (1990) *Methods Enzymol.* **182**, 425–441
42. Harlow, E., and Lane, D. (1988) *Antibodies: A Laboratory Manual*, Cold Spring Harbor Laboratory, Cold Spring Harbor, New York
43. Scatchard, G. (1949) *Ann. N. Y. Acad. Sci.* **51**, 660–672
44. Sugarman, B. J., Aggarwal, B. B., Hass, P. E., Figari, I. S., Palladino, M. A., and Shepard, H. M. (1985) *Science* **230**, 943–945
45. Aggarwal, B. B. (1992) in *Tumor Necrosis Factors: Structure, Function and Mechanism of Action* (Aggarwal, B. B., and Vilcek, J., eds) pp. 61–92, Marcel Dekker, Inc., New York
46. McFadden, G., and Graham, K. (1994) *Semin. Virology* **5**, 421–429
47. McFadden, G., Graham, K., Ellison, K., Barry, M., Macen, J., Schreiber, M., Mossman, K., Nash, P., Lalani, A., and Everett, H. (1995) *J. Leukocyte Biol.* **57**, 731–738
48. Rothe, J., Gehr, G., Loetscher, H., and Lesslauer, W. (1992) *Immunol. Res.* **11**, 81–90
49. Pennica, D., Lam, V. T., Mize, N. K., Weber, R. F., Lewis, M., Fendly, B. M., Lipari, M. T., and Goeddel, D. V. (1992) *J. Biol. Chem.* **267**, 21172–21178
50. Lewis, M., Tartaglia, L. A., Lee, A., Bennett, G. L., Rice, G. C., Wong, G. H. W., Chen, E. Y., and Goeddel, D. V. (1991) *Proc. Natl. Acad. Sci. U. S. A.* **88**, 2830–2834
51. Loetscher, H., Gentz, R., Zulauf, M., Lustig, A., Tabuchi, H., Schlaeger, E.-J., Brockhaus, M., Gallati, H., Manneberg, M., and Lesslauer, W. (1991) *J. Biol. Chem.* **266**, 18324–18329
52. Goodwin, R. G., Anderson, D., Jerzy, R., Davis, T., Brannan, C. I., Copeland, N. G., Jenkins, N. A., and Smith, C. A. (1991) *Mol. Cell. Biol.* **11**, 3020–3026
53. Pennica, D., Kohr, W. J., Fendly, B. M., Shire, S. J., Raab, H. E., Borchardt, P. E., Lewis, M., and Goeddel, D. V. (1992) *Biochemistry* **31**, 1134–1141
54. Debets, R., and Savelkoul, H. F. J. (1994) *Immunol. Today* **15**, 455–458
55. Fountoulakis, M., Juranville, J.-F., Stuber, D., Weibel, E. K., and Garotta, G. (1990) *J. Biol. Chem.* **265**, 13268–13275
56. Smith, R. A., and Baglioni, C. (1992) in *Tumor Necrosis Factors: Structure, Function, and Mechanism of Action* (Aggarwal, B. B., and Vilcek, J., eds) pp. 131–147, Marcel Dekker, Inc., New York
57. Thoma, B., Grell, M., Pfizenmaier, K., and Scheurich, P. (1990) *J. Exp. Med.* **172**, 11019–1023
58. Tartaglia, L. A., and Goeddel, D. V. (1992) *J. Biol. Chem.* **267**, 4304–4307
59. Wong, G. H. W., Tartaglia, L. A., Lee, M. S., and Goeddel, D. V. (1992) *J. Immunol.* **149**, 3350–3353
60. Marsters, S. A., Frutkin, A. D., Simpson, N. J., Fendly, B. M., and Ashkenazi, A. (1992) *J. Biol. Chem.* **267**, 5747–5750
61. Shakhow, A. N., Kuprash, D. V., Azizov, M. M., Jongeneel, C. V., and Nedospasov, S. A. (1990) *Gene (Amst.)* **95**, 215–221
62. Hale, K. K., Smith, C. G., Baker, S. L., Vanderslice, R. W., Squires, C. H., Gleason, T. M., Tucker, K. K., Kohno, T., and Russell, D. A. (1995) *Cytokine* **7**, 26–38
63. Ashkenazi, A., Marsters, S. A., Capon, D. J., Chamow, S. M., Figari, I. S., Pennica, D., Goeddel, D. V., Palladino, M. A., and Smith, D. H. (1991) *Proc. Natl. Acad. Sci. U. S. A.* **88**, 10535–10539
64. Higuchi, M., and Aggarwal, B. B. (1992) *J. Biol. Chem.* **267**, 20892–20899
65. Tartaglia, L. A., Pennica, D., and Goeddel, D. V. (1993) *J. Biol. Chem.* **268**, 18542–18548
66. Smith, C., and Goodwin, R. G. (1995) in *Viroceptors, Virokines and Related Immune Modulators Encoded by DNA Viruses* (McFadden, G., ed) pp. 29–40, R. G. Landes Co., Austin
67. Olsson, I., Gatanaga, T., Gullberg, U., Lantz, M., and Granger, G. A. (1993) *Eur. Cytokine Netw.* **4**, 169–180
68. Howard, O. M., Clouse, K. A., Smith, C., Goodwin, R. G., and Farrar, W. L. (1993) *Proc. Natl. Acad. Sci. U. S. A.* **90**, 2335–2339
69. Haak-Fredenscho, M., Marsters, S. A., Mordenti, J., Brady, S., Gillett, N. A., Chen, S. A., and Ashkenazi, A. (1994) *J. Immunol.* **152**, 1347–1353
70. Peppel, K., Crawford, D., and Beutler, B. (1991) *J. Exp. Med.* **174**, 1483–1489
71. Butler, D. M., Scallion, B., Meager, A., Kissnerghis, M., Corcoran, A., Chernajovsky, Y., Feldmann, M., Ghayeb, J., and Brennan, F. (1994) *Cytokine* **6**, 616–623
72. Bazzoni, F., Alejos, E., and Buelter, B. (1995) *Proc. Natl. Acad. Sci. U. S. A.* **92**, 5376–5380
73. Declercq, W., Vandenebeele, P., and Fiers, W. (1995) *Cytokine* **7**, 701–709